Nanoscale

Accepted Manuscript

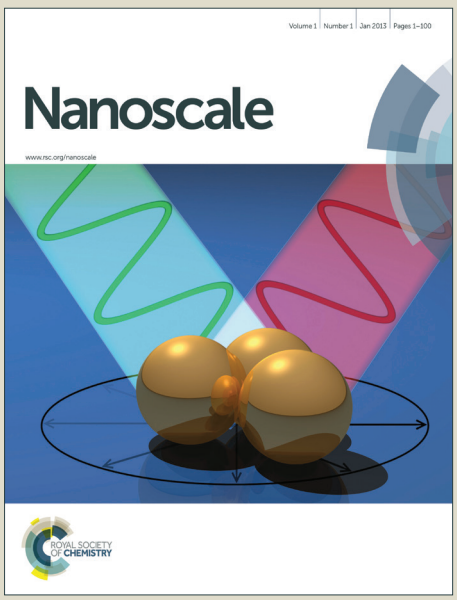

ROYAL SOCIETY OF CHEMISTRY

www.rsc.org/nanoscale

Nanoscale

RSCPublishing

ARTICLE

Facile Synthesis of Dumbbell-Shaped Multi-Compartment Nanoparticles

Cite this: DOI: 10.1039/x0xx00000x

Karla Doermbach,[a] Andrij Pich[a,]*

Received 00th January 2012,
Accepted 00th January 2012

DOI: 10.1039/x0xx00000x

www.rsc.org/

In this article we report on the controlled synthesis of asymmetric lemon-shaped and dumbbell-shaped multi-compartment nanoparticles (MCPs) with reactive surface and interesting morphology. In our approach we utilize partial coating of hematite ellipsoids with a hydrophobic polymer layer followed by selective silica deposition on the non-coated surface. Ellipsoidal hematite particles provide a non-centric asymmetry, which is strongly enhanced during the seeded emulsion polymerization. The asymmetric growth of polymer on the hematite particle surface is driven by phase separation phenomena, which lead to a reduction of the interfacial tension. We found the tips of the hematite ellipsoids to be uncovered after polymerization. A selective deposition of silica onto the free tips leads to dumbbell-shaped particles with hydrophilic and hydrophobic parts.

Introduction

Bottom-up synthesis of MCPs has moved into the focus of scientist since many years now. [1] Recently many studies have been performed in this field to design nanosized and multi-functional building blocks. Those complex structures can find possible applications in field of self-assembly[2, 3], nano/opto-electronics[4, 5], catalysis[6], sensor technology and biomedicine[7, 8]. Especially the design of very complex nano-architectures obtained directly from solution and further more scaling up the syntheses are very challenging tasks. [9, 10] For the formation of Janus-faced nanoparticles several mechanisms have been proposed, including selective surface modification[11], polymer-based direct synthesis[9, 12] and phase separation on particle surfaces[13]. Among spherical or core-shell particles, nanoparticles with less symmetry, e.g. lemon-shaped particles or dumbbells[14, 15], are of particular interest. All methods proposed so far to synthesize dumbbell structures describe a preferential asymmetrical overgrowth of a second component on a previously formed seed particle.[16] Especially the control of morphology during synthesis of MCPs composed of organic and inorganic components remains challenging.[17] It seems trivial, but this asymmetric growth needs to be energetically favoured compared to symmetric growth or a separate nucleation.[16]

Besides the direct contact of two or more components providing multiple physical and chemical functionalities, dumbbell-shape nanoparticles offer additional features due to their special shape. In several studies it was shown that asymmetric MCPs can be assembled into even more complex structures.[18, 19] The problem addressed in those studies is related to the need of assembling MCPs in well-defined geometries. The aim is to build up active devices, e.g. sensors or solar cells, right from the nanoscale in the future. For a high stability of formed structures it is of high importance to introduce binding sides where molecules can be attached to fix the assembled pattern.[20]

However, easy and reproducible synthetic approaches, which enable up-scaling, for those building blocks are still rarely to find in the literature. In this article we establish a simple and robust method for synthesis of lemon-shape and dumbbell-like nanoparticles by bottom-up solution approach. In a first step a co-polymer composed of poly(styrene-*co*-glycidyl methacrylate-*co*-divinylbenzene) (PSGD) is deposited onto the ellipsoidal nanoparticle using a seeded polymerization technique. Afterwards, dumbbell-shaped MCPs were formed by controlled deposition of silica onto the uncoated tips of hematite. The selectivity of this reaction is induced by the preferred affinity of silica to bind onto hematite rather than onto PSGD.[21, 22]

Experimental

Materials

Iron (III) chloride hexahydrate (99%, Merck), sodium dihydrogen phosphate monohydrate (99%, Merck), 16-heptadecenoic acid (Aaron Chemistry GmbH), ammonia solution (25% aqueous solution, KMF), divenylbenzene (DVB) (Sigma-Aldrich), potassium persulfate (Sigma-Aldrich) and ethanol (p.a., VWR) were used as delivered. Styrene and glycidyl methacrylate (GMA) were received by Sigma-Aldrich and were purified by distillation.

Synthesis of Hematite (α-Fe_2O_3) Nanoparticles

The synthesis of ellipsoidal hematite nanoparticle can be found elsewhere.[23] For the synthesis 1,000 mL of a 0.02 M $FeCl_3$ solution containing NaH_2PO_4 in a concentration of $4.5 \cdot 10^{-4}$ M was heated to boiling point under reflux conditions. The solution was kept at boiling point for the next 48 h. Afterwards, the dispersion was cooled down to room temperature The particles were collected by centrifugation. In a next step, the

excess of ions was removed by repeated washing with de-ionized water.

Functionalization of Hematite (α-Fe_2O_3) Nanoparticles and Synthesis of Asymmetric Hematite/ Polymer MCPs (α-Fe_2O_3@PSGD)

According to the synthetic procedure proposed by *M. Feyen et al.*[9] the particles surface was functionalized and further modified.

Therefore, 33 mg of α-Fe_2O_3 nanoparticles were mixed with 7.5 mL ammonia solution (1.3% NH_3 in water) containing 0.15 mmol of 16-heptadecenecarboxylic acid for 30 min at 50°C.

All reactions are performed under nitrogen atmosphere. For synthesis of asymmetric α-Fe_2O_3@PSGD colloids, 33 mg of functionalized α-Fe_2O_3 nanoparticles were stirred with appropriate amount of monomers for 1 min at 50°C. Amounts of co-monomer can be found in Table 1. Afterwards, the reaction mixture was diluted with 71 mL of warm ammonia solution (1.3% NH_3 in water) and then heated to 70°C. $K_2S_2O_8$ (KPS) was dissolved in 1 mL water and added to the reaction to initiate the polymerization. The temperature was kept constant overnight. Next day a stable reddish dispersion was obtained. For further purification the dispersion was cooled to room temperature and centrifuged for 10 min with a centrifugation speed of 12,900 rcf followed by redispergation of the sediment in de-ionized water. Particles were centrifuged and washed with de-ionized water five times. The obtained hybrid colloids were finally dispersed in de-ionized water.

Table 1. Amounts of monomers (GMA, styrene and DVB) and initiator (KPS) used for synthesis of MCPs.

Sample	GMA [mmol]	Styrene [mmol]	DVB [mmol]	KPS [mmol]
α-Fe_2O_3@PSGD-1	4.95	4.95	2.95	0.09
α-Fe_2O_3@PSGD-2	9.90	9.90	5.90	0.17
α-Fe_2O_3@PSGD-3	19.80	19.80	11.80	0.34

Selective Silica Deposition on α-Fe_2O_3@PSGD nanocomposites

In a typical procedure, 2.5 mL of an aqueous solution containing 8.3 mg α-Fe_2O_3@PSGD-2 were mixed with 1.55 mL ammonia solution (1.2 vol-%) and 1.55 mL ethanol for 1 h. Following 6.25 mL ethanol were mixed with 0.29 mL ammonia solution (25 vol-%) and were added to the reaction mixture. Furthermore, a solution of TEOS in 4.4 mL ethanol was added rapidly to the dispersion. Three different amounts of TEOS (31 µL, 62 µL and 93 µL) were used. The samples are named as follows: α-Fe_2O_3@PSGD-2@SiO_2-1 (31 µL TEOS), α-Fe_2O_3@PSGD-2@SiO_2-2 (62 µL TEOS) and α-Fe_2O_3@PSGD-2@SiO_2-3 (93 µL TEOS). Reaction was kept stirring for 24 h at room temperature. Samples were purified by repeated centrifugation and washing with distilled water.

Characterization Techniques

Transmission electron microscopy (TEM) was measured on Zeiss LibraTM 120 (Carl Zeiss, Oberkochen, Germany). The electron beam accelerating voltage was set at 120 kV. A drop of the sample was trickled on a piece of formvar and carbon coated copper grid. Before being placed into the TEM specimen holder, the copper grid was air-dried under ambient conditions.

Fourier transform infrared (FTIR) spectra were recorded using a Nexus 470 (Thermo Nicolet). Samples were dried and measured in KBr.

The thermogravimetrical analysis (TGA) was performed using a Netsch TG 209C. Before measuring samples were dried in vacuum for 48 h. All samples were analyzed from 25-500°C at a heating rate of 10 °C/min in nitrogen atmosphere.

Field emission scanning electron microscopy (FE-SEM) images and energy dispersive X-ray spectroscopy (EDX) analysis were obtained in a Hitachi SU9000 (Tokyo, Japan) electron microscope using a beam voltage of 30 kV and AZtec control software (Version 2.2, Oxford Instruments GmbH). The EDX maps were recorded with acquisition times larger than 30 min. A BF-STEM detector and a SE detector were used parallel to detect SEM and TEM images at the same time. For sample preparation one droplet of the dispersion was applied onto a copper grid, which was covered with a perforated carbon film.

Zeta potential measurements were performed on highly diluted dispersion of nanoparticles using a ZetaSizer Nano ZS (Malvern Instruments, Worcestershire, UK). For the measurement one droplet of the particular dispersion was dropped into 5 mL distilled water with (pH 7).

Results and Discussion

Synthetic Route

In this study we investigated the targeted formation of lemon and dummbell-shaped MCPs. Firstly, we succeeded in the template-directed synthesis of α-Fe_2O_3@PSGD nanoparticles. These particles consist of a inorganic hematite ellipsoidal shaped core and an asymmetric organic polymer coating composed of several monomers with different chemical polarity.

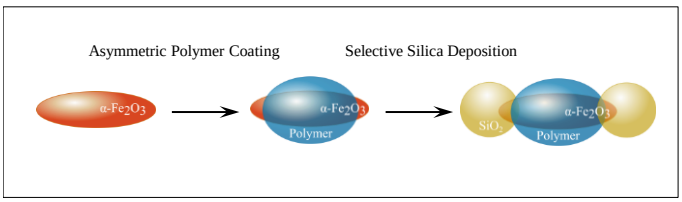

Scheme 1. Simplified synthesis route to lemon-shaped and dumbbell-shape MCPs.

Scheme 1 illustrates the synthetic pathway. Before an asymmetric polymer coating can be performed ellipsoidal hematite nanoparticles need to be pre-funcitonalized by 16-heptadecarboxylic acid acting as a intermediator for the solubilisation of monomers as well as a binding side for the polymer to the particle at the same time. For the asymmetric coating it is essential that the monomer mixture is predominatly hydrophobic. If the monomers are water soluble we observed a uniform shell formation around α-Fe_2O_3 core. Here, styrene is used as a hydrophobic monomer, DVB is used as a crosslinker and GMA is supposed to be located on the water/monomer interface improving colloidal stability of the hematite/monomer system. Furthermore, the hematite nanoparticles are partically coated with the reactive copolymer ehxibiting epoxy groups by seeded polymerisation approach. It was found that the edges of the nanoparticles are partically free from polymer offering the possibility for further modifications. Silica was deposited selectively in a base catalyzed process from an ethanolic solution on the free tips forming caps.

Characterization

TEM analysis is a very useful tool to observe the structure of asymmertric MCPs thoroughly. Based on the considerable diffrence in atomic number of inorganic and organic materials, the core

material, hematite, appears dark and accordingly the polymer coating appears lighter. This effect offers a direct method to characterize the structure of the particles. Uncoated hematite ellipsoids show a logitudinal axis of about 215 ± 36 nm and a transversal axis 59 ± 9 nm. After polymerization of PSGD onto the hematite nanoparticle surfaces the composite material was analyzed by TEM in detail. Figure 1 shows a concentration series of different ratios of hematite nanoparticles to monomer during synthesis. For the lowest polymer to nanoparticle ratio only few discrete polymer "patches" were visible on the surface of the α-Fe_2O_3 ellipsoids (Figure 1a). A uniform deposition of polymer onto the surface was observed when we doubled the amount of monomers during synthesis (Figure 1b). Further increase of the monomer concentration leads to undesirable formation of secondary polymer particles (Figure 1c). Figure 1b indicates clearly that the edges of the hematite nanoellipsoids are not covered with polymer layer. We found that polymer layer is covalently attached to the hematite surface. The attempt to remove polymer by extraction was not successful (Supporting Information).

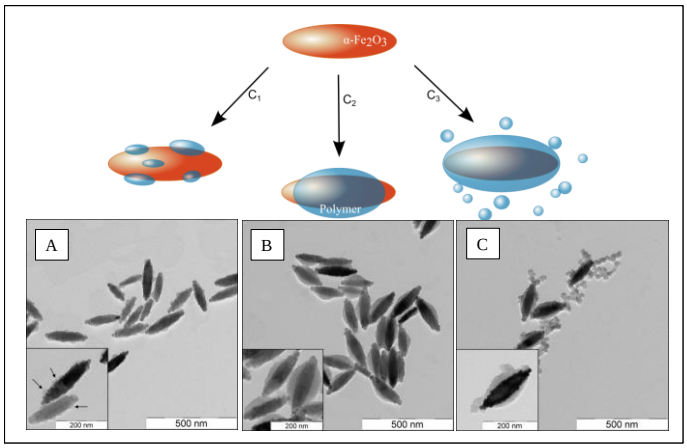

Figure 1. Dependence of monomer concentration on asymmetric polymer coating process of ellipsoidal hematite nanoparticles: a) α-Fe_2O_3@PSGD-1; b) α-Fe_2O_3@PSGD-2 and c) α-Fe_2O_3@PSGD-3.

In the next step silica was deposited selectively on the edges of the ellipsoids to obtain dumbbell-shaped MCPs. We synthesized a series of MCPs by varying silica amounts. Sample α-Fe_2O_3@PSGD-2@SiO_2-1 was analyzed by FE-SEM, STEM and EDX analysis simultaneously. The TEM analysis results for samples α-Fe_2O_3@PSGD-2@SiO_2-2 and α-Fe_2O_3@PSGD-2@SiO_2-3 can be found in the Figure 2.

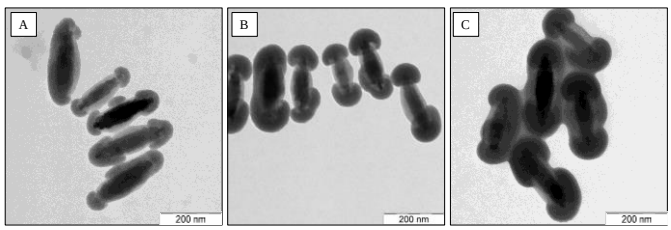

Figure 2. TEM images of hematite-polymer hybrid particles coated with different amounts of silica: a) α-Fe_2O_3@PSGD-2@SiO_2-1; b) α-Fe_2O_3@PSGD-2@SiO_2-2 and c) α-Fe_2O_3@PSGD-2@SiO_2-3.

Here, TEM images of a series of samples where the silica concentration was increased steadily during the silica deposition. It can be seen that in a first step the cap starts to grow (Figure 2a/ b) until the caps touch each other and start to form a shell (Figure 2c). TEM images indicate a clear border between SiO_2 and PS phases reflected in the contrast difference. Therefore, based on this experimental results we conclude that SiO_2 deposits predominantly of the PS-free tips of α-Fe_2O_3 ellipsoids.

Figure 3a shows a FE-SEM overview image of the sample. It is clearly visible that almost all MCPs are dumbbell-shaped. A closer look is given by Figure 3b-d showing FE-SEM, STEM and EDX mapping for the same image. The combination of the three methods give information about the three dimensional shape (FE-SEM), as well as the distribution of materials (STEM and EDX). The EDX image shows clearly where the three main elements iron (yellow), silicon (red), and carbon (blue) used are located. The aggregation and overlap of the nanoparticles on the microscopy grids after drying process makes EDX analysis difficult and judgment of the element distribution based on Figure 3d becomes questionable. However, by analyzing nanoparticles that are separated from their neighbors and taking into account the TEM images in Figure 2 one may conclude that SiO_2 deposits predominantly on the tips of ellipsoids with extremely high efficiency (our estimation is that more that 95% silica is deposited on the tips of ellipsoids). The visualization of some SiO_2 deposited on the PS-coated sides of ellipsoids was not possible due to the resolution limit of the instrument and contamination of the TEM grids with Si. From this we conclude that the amount of SiO_2 deposited on the PS-coated parts is extremely low and below the detection limit of the EDX detector.

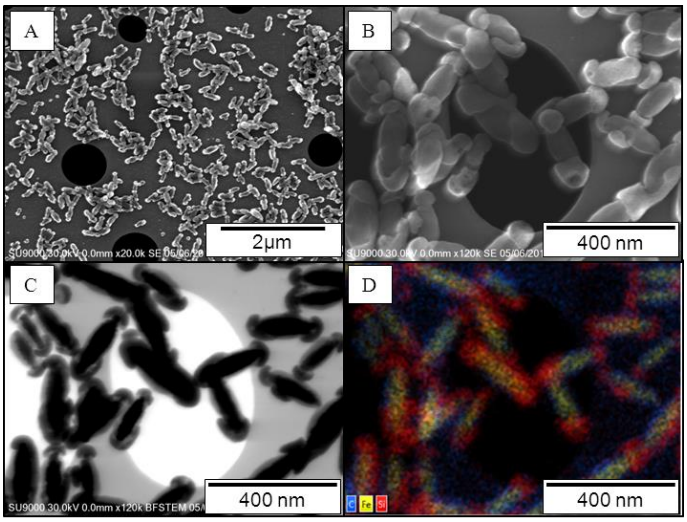

Figure 3. FE-SEM of α-Fe_2O_3@PSGD-2@SiO_2-1 a) overview; b) detailed FE-SEM image; c) STEM image and c) EDX mapping for sample α-Fe_2O_3@PSGD-2@SiO_2-1.

The results obtained by EDX mapping can be further confirmed by FTIR spectroscopy. Characteristic peaks were found for hematite, the polymer and silica for the different MCPs. Figure 4a shows FTIR spectra comparing samples of α-Fe_2O_3, α-Fe_2O_3@PSGD-2 and α-Fe_2O_3@PSGD-2@SiO_2-1. Peaks at 584 and 482 cm^{-1} are characteristic for hematite.[24] Peaks in the region from 3083 to 3023 cm^{-1} can be assigned to the C-H stretching of the benzene rings referring to styrene and divinylbenzene. Further stretching vibrations were found for the CH_3 group at 2925 and 2852 cm^{-1}. A very small peak was detected at 1727 cm^{-1}. This peak is related to the C=O stretching of the carbonyl group referring to GMA. A broad peak around 1630 cm^{-1} can also be assigned to the aromatic rings, but is also typical for hematite. Presumably several peaks are overlaid in this part of the spectrum making the detection of characteristic groups challenging in this region. Peaks at lower wavenumbers can be clearly assigned to hematite. After silica

deposition a very strong peak at 1099 cm^{-1} can be detected. Another characteristic signal can be attributed to the –Si–OH vibration at 931 cm^{-1}.[25, 26]

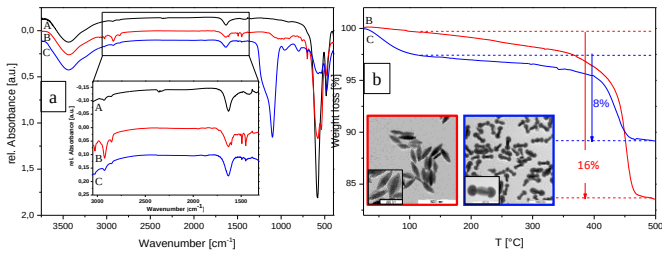

Figure 4. a) FTIR spectra of α-Fe_2O_3 (black, A), α-Fe_2O_3@PSGD-2 (red, B) and α-Fe_2O_3@PSGD-2@SiO_2-1 (blue, C) (inset shows spectral region 3000-1500 cm^{-1} for better comparison); b) TGA curves for α-Fe_2O_3@PSGD-2 (red, B) and α-Fe_2O_3@PSGD-2@SiO_2-1 (blue, C) with TEM images of both samples.

TGA measurements were performed to determine the polymer content in multicomponent nanoparticles by measuring the weight loss. A continuous increase of polymer amount was measured for samples α-Fe_2O_3@PSGD-1 to α-Fe_2O_3@PSGD-3. The ideal ratio of hematite to PSGD was found to be 5:1. After silica deposition a ratio of hematite to PSGD to silica was calculated to be 5:1:6 for ideal shaped MCPs.

Table 2. Weight fractions of hematite ($Wt_{\alpha\text{-}Fe2O3}$), polymer ($Wt_{Polymer}$) and silica (Wt_{SiO2}) and zeta potential (ξ) of lemon-shaped and dumbbell-shaped particles measured at pH 7.

Sample	$Wt_{\alpha\text{-}Fe2O3}$ [%]	$Wt_{polymer}$ [%]	Wt_{SiO2} [%]	ζ [mV]
α-Fe_2O_3	100	0	0	+3.1 ± 7.1
α-Fe_2O_3@PSGD-1	85	15	0	-37.6 ± 5.3
α-Fe_2O_3@PSGD-2	84	16	0	-38.6 ± 5.5
α-Fe_2O_3@PSGD-3	67	33	0	-36.4 ± 7.5
α-Fe_2O_3@PSGD-2@SiO_2-1	68	13	19	-42.4 ± 10.3
α-Fe_2O_3@PSGD-2@SiO_2-2	58	11	31	-50.2 ± 9.9
α-Fe_2O_3@PSGD-2@SiO_2-3	42	8	50	-54.9 ± 12.8

In addition to the other methods used, zeta potential measurements are useful to follow the surface modification. At pH 7 hematite nanoparticles are known to have a point of zero charge. After coating with PSGD the zeta potential drops to negatives value around -36 to -38 mV for all lemon-shaped samples. The negative charge of PSGD can be attributed to residues of the negatively charged initiator introduced during the polymerization. After silica deposition the zeta potential becomes even more negative. With increasing amount of silica the zeta potential increases to -55mV for dumbbell-shaped MCPs. All values are summarized in Table 2. In summary, we developed a simple and robust bottom-up method for the synthesis of composite colloids with complex shapes. This methodology can be easily extended to integrate different chemical functionalities and combine different materials on the nanoscale.

Conclusions

In this work we established a directed synthesis of multi-compartment particles (MCPs) with complex shapes from aqueous solution. The synthesis approach was based on phase separation phenomena that occur on the nanoparticle surface due to differences in polarity of the used monomers and precursors. It was shown that there is an optimal ratio of ellipsoidal hematite nanoparticle to monomer during the synthesis to obtain uniformly coated particles showing a strong asymmetry reflected in non-coated edges. Furthermore, the selective deposition of silica onto the free edges of α-Fe_2O_3@PSGD nanoparticles resulted in dumbbell-shaped nanoparticles. These structures are supposed to be amphiphilic due to the hydrophobic polymer and the hydrophilic silica parts. We found the MCPs to be colloidally stable in water as well as in organic solvents e.g. THF or acetone.
Due to similar surface properties, we expect that this synthetic strategy will be applicable to other iron oxides e.g. magnetite and maghemite. The requirements to the core material are: a) colloidal stability of the nanoparticles in water and b) the surface should be accessible for the modification with 16-heptadecenoic acid. The dumbbell-shaped MCPs could be used as nanoscale building blocks in assembly processes. By dissolving the hematite core MCPs could be transferred to hollow capsules and use them as carriers. The hydroxyl-groups on the silica caps as well as epoxy groups on the polymer surface offer the possibility to modify the MCPs further. Silica caps could be decorated with functional silanes to introduce various functionalities like amine, vinyl or thiol groups. Epoxy groups anchored to the polymer coating of MCPs can directly react with amines or thiols acting as anchor groups for binding proteins, florescent dyes or polymers.

Acknowledgements

KD and AP thank Volkswagen Foundation for financial support of this research. The authors would also like to thank David Schroeter, Dr. Sebastian Lecher and Sabrina Mallmann for support with FE-SEM, STEM and EDX measurements and Dr. Walther Tillmann for support with FTIR measurements.

Notes

[a] Functional and Interactive Polymers, DWI- Leibniz Institute for Interactive Materials, Institute of Technical and Macromolecular Chemistry, RWTH Aachen University, Forckenbeckstrasse 50, D-52056 Aachen, Germany

Electronic Supplementary Information (ESI) available: TEM images of silica coating without polymer layer, experiments for removal of polymer by solvent extraction, TEM images of spherical α-Fe_2O_3 nanoparticles with an asymmetric PSGD coating, and additional FESEM, TEM/EDX images of α-Fe_2O_3@PSGD-2@SiO_2 nanoparticles See DOI: 10.1039/b000000x/

References

1 S. C. Glotzer, M. J. Solomon, *Nat. Mater.*, 2007, **6**, 557.
2 N. Glaser, D. J. Adams, A. Boker, G. Krausch, *Langmuir*, 2006, **22**, 5227.
3 J. He, M. J. Hourwitz, Y. Liu, M. T. Perez, Z. Nie, *Chem. Commun.*, 2011, **47**, 12450.
4 S. Gangwal, O. J. Cayre, O. S. Valev, *Langmuir*, 2008, **24**, 13312.
5 T. Nisisako, T. Torii, T. Takahashi, Y. Takizawa, *Adv. Mater.*, 2006, **18**, 1152.
6 S. Cossley, J. Faria, M. Shen, D. E. Resasco, *Science*, 2010, **327**, 68.
7 J. He, Y. Liu, T. C. Hood, P. Zhang, J. Gong, Z. Nie, *Nanoscale*, 2013, **5**, 5151.
8 A. Walther, A. H. E. Müller, *Soft Matter*, 2008, **4**, 663 .

9 M. Feyen, C. Weidenthaler, F. Schüth, A.-H. Lu, , *J. Am. Chem. Soc.*, 2010, **132**, 6791.
10 J. Du, R. K. O´Reilly, *Chem. Soc. Rev.*, 2011, **40**, 2402.
11 M. Lattuada, T. A. Hatton, *J. Am. Chem. Soc.*, 2007, **129**, 12878.
12 J. Ge, Y. Hu, T. Zhang, Y. Yin, *J. Am. Chem. Soc.*, 2007, **129**, 8974.
13 T. Chen, M. Yang, X. Wang, L. H. Tan, H. Chen, *J. Am. Chem. Soc.*, 2008, **130**, 11858.
14 F. Chu, M. Siebenbürger, F. Polzer, C. Stolze, J. Kaiser, M. Hoffmann, N. Heptner, J. Dzubiella, M. Drechsler, Y. Lu, M. Ballauff, *Macromol. Rapid Commun*., 2012, **33**, 1042.
15 H. Yu, M. Chen, P. M. Rice, S. X. Wang, R. L. White, S. Sun, *Nano Lett.*, 2005, **5**, 379.
16 S. Jiang, S. Granick, Janus particle synthesis, self-assembly and applications, *The Royal Society of Chemistry*, 2012, 29-53.
17 J. He, M. T. Perez, P. Zhang, Y. Liu, T. Babu, J. Gong, Z. Nie, *J. Am. Chem. Soc*., 2012, **134**, 3639.
18 K. Liu, Z. H. Nie, N. N. Zhao, W. Li, M. Rubinstein, E. Kumacheva, *Science*, 2010, **329**, 197.
19 Z. H. Nie, D. Fava, E. Kumacheva, S. Zou, G. C. Walker, M. Rubinstein, *Nat. Mater*., 2007, **6**, 609.
20 P. D. Cozzoli, L. Manna, *Nat. Mater*., 2005, **4**, 801.
21 Y. Lu, Y. Yin, B. T. Mayers, Y. Xia, *Nano Lett.*, 2002, **2**, 183.
22 I. Tissot, J. P. Reymond, F. Lefebvre, E. Bourgeat-Lami, *Chem. Mater*., 2002, **14**, 1325.
23 a) K. Dörmbach, G. Agrawal, S. Thies, M. Servos, U. Klemradt, A. Pich, *Part. Part. Syst. Charact.*, 2014, **31**, 365.; b) M. Ozaki, S. Kratohvil, E. Matijevic, *J. Colloid Interface Sci.*, 1984, **102**, 146.
24 I. J. Bruce, J. Taylor, M. Todd, M. J. Davies, E. Borioni, C. Sangregorio, T. Sen, *J. Magn. Magn. Mater*., 2004, **284**, 145.
25 P. Vejayakumaran, I. A. Rahmana, C. S. Sipaut, J. Ismail, C. K. Chee, *J. Colloid Interface Sci.*, 2008, **328**, 81.
26 N. Frickel, R. Messing, T. Gelbrich, A. M. Schmidt, *Langmuir*, 2010, **26**, 2839.